

## Changes in Physical Properties of a Compost Biofilter Treating Hydrogen Sulfide

Juan M. Morgan-Sagastume , Adalberto Noyola , Sergio Revah & Sarina J. Ergas

To cite this article: Juan M. Morgan-Sagastume , Adalberto Noyola , Sergio Revah & Sarina J. Ergas (2003) Changes in Physical Properties of a Compost Biofilter Treating Hydrogen Sulfide, Journal of the Air & Waste Management Association, 53:8, 1011-1021, DOI: [10.1080/10473289.2003.10466249](https://doi.org/10.1080/10473289.2003.10466249)

To link to this article: <https://doi.org/10.1080/10473289.2003.10466249>



Published online: 22 Feb 2012.



Submit your article to this journal [↗](#)



Article views: 360



View related articles [↗](#)



Citing articles: 34 View citing articles [↗](#)

# Changes in Physical Properties of a Compost Biofilter Treating Hydrogen Sulfide

**Juan M. Morgan-Sagastume and Adalberto Noyola**

*Institute of Engineering, National Autonomous University, Mexico City, Mexico*

**Sergio Revah**

*Processes and Hydraulics Department, Metropolitan Autonomous University, Iztapalapa, Mexico*

**Sarina J. Ergas**

*Department of Civil and Environmental Engineering, University of Massachusetts, Amherst, Massachusetts*

## ABSTRACT

A technique is presented that can be used to estimate the changes in physical structure in a natural biofilter packing medium, such as compost, over time. The technique applies information from tracer studies, grain size distribution, and pressure drop analysis to a model that estimates the number of channels, average channel diameter, number of particles, and specific surface area of the medium. Important operational factors, such as moisture content, pressure drop, and sulfate accumulation also were evaluated both in a conventionally operated biofilter and in one operated with periodic compost mixing. In the conventionally operated laboratory-scale compost biofilter, hydrogen sulfide ( $H_2S$ ) removal efficiency decreased from 100% to ~90% over 206 days of operation. In a similar system, operated with compost mixing, the  $H_2S$  removal efficiency was maintained near 100%. Variations in media moisture conditions and specific surface area can explain the results observed in this study. Under conventional operation, drying near the inlet disintegrated the compost particles, producing a large number of particles and flow channels and increasing the specific surface area. At

the top of the column, where moisture was added, particle size increased and specific surface area decreased. In the column with media mixing, moisture content, particle size, and specific surface area remained homogeneous.

## INTRODUCTION

Compost-based biofiltration is one of the most important biological processes applied to treat waste gases and to control odors. This system is based on the interaction of gas-phase pollutants in an organic media, such as compost. The degradation activity derives from microorganisms that live and develop in the media. Undesirable compounds in the gas are absorbed and degraded by the microorganisms.

Three important general factors that determine compost biofilter performance are (1) the quality of the filter media (including temperature, void fraction, particle size, moisture content, microbial diversity, and nutrients), (2) the prevailing conditions of gas flow inside the biofiltration unit (including superficial velocity, gas distribution, and inlet pressure), and (3) the substrate solubility, degradability, and loading rate applied. Research efforts must be focused on the biofilter media to upgrade the performance of compost biofilters. Biofilters are living pollution control systems and are subject to dynamic changes. Experimental data<sup>1–5</sup> show an initial increase and subsequent drop in contaminant removal efficiency, especially in biofilters that are operated for a long time. The initial improvement in performance can be explained by growth and acclimation of the microbial population.<sup>6,7</sup> Alonso et al.<sup>2</sup> stated that the key reason for the subsequent drop in removal efficiency is the reduction in the specific surface area of the biofilm caused by biomass accumulation. However, in compost biofilters, the specific

## IMPLICATIONS

Over long periods of operation, the removal efficiency of conventionally operated compost biofilters decreases because of drying, channeling, and reduction in specific surface area. The results of this research demonstrate that, using media mixing, the removal efficiency can be maintained near 100%. To avoid channeling, as well as to achieve constant media moisture content, particle size and gas distribution, void fraction, and general homogeneity, periodic media mixing with controlled water addition is recommended.

surface area can decrease, independent of biomass accumulation, because of channeling, media compaction, drying, and particle agglutination. As the media undergo these processes, there is a gradual decrease in the specific surface area and a decrease in gas retention time. A number of studies have shown that media mixing can restore biofilter performance in aged systems by decreasing channeling, improving gas distribution, and by controlling moisture.<sup>8-13</sup>

A number of mathematical models have been developed to describe the internal physical, chemical, and biological processes that occur in a biofilter. Some of these models analyze substrate removal using first-order kinetics under steady-state conditions.<sup>1,14,15</sup> Other kinetic models take into account the substrate mass transfer from the gas phase to the biofilm, simultaneously considering convection, diffusion, and reaction under either steady-state or dynamic conditions.<sup>16</sup> Other models have been developed that consider the addition of activated carbon,<sup>17,18</sup> the influence of oxygen concentration,<sup>19</sup> and substrate adsorption on bed particles.<sup>20,21</sup> Zarook et al.<sup>10</sup> presented a model that can be used under dynamic conditions where gas axial dispersion effects, adsorption of substrate onto the packing material, and the potential limiting effects of oxygen were considered. These models can be fit to substrate removal profiles and provide general information about whether the reaction rate is zero or first-order and whether the degradation process is kinetic or mass transfer-limited. Models have also been developed that give information about the internal changes in the biofilter media, such as substrate adsorption capacity, formation of biolayers around solid particles, and biolayer thickness.<sup>2,13,22</sup> However, these models do not consider parameters related to the internal physical structure, such as the number of particles, particle size distribution, number of flow channels, and channel size.

The objective of this project is to describe the changes in media physical structure in compost biofilters treating hydrogen sulfide (H<sub>2</sub>S). A model was developed that estimates the number of particles, number of flow channels, average channel size, and specific surface area in a packed bed. Pressure drop, particle size distribution, and tracer studies were performed periodically to calibrate the model. In addition, the effect of media mixing on the maintenance of media physical structure and biofilter performance was evaluated.

## THEORETICAL DEVELOPMENT

The flow channel model developed during this study estimates the number of particles, number of flow channels, average channel size, and specific surface area in a packed bed. The model assumes uniformly shaped solids that are defined by particle diameter, sphericity, and bed void

fraction. The model does not take into account biomass growth or particle arrangement in the bed. The flow channel model is based on four equations: two for specific surface area; one that allows the estimation of channel diameter based on a series of parallel, cylindrical channels in the bed; and one for average and sieve particle diameter as a function of sphericity. Pressure drop profiles and the average retention time of an inert tracer were used to estimate average particle diameter and void fraction, respectively.

### Flow Channel Model

This mathematical model is based on a conceptual model of the packed bed as a series of parallel, cylindrical channels that carry the gas flow from the inlet to the outlet of the biofilter. Assuming that the external area of the channels is equal to the area of the particles in the bed and the void volume of the bed is equal to the sum of the volumes of all the channels, the following equation can be used to calculate  $d_c$  (m), the diameter of the channels:<sup>23</sup>

$$d_c = \frac{2}{3} \phi d_p \frac{\varepsilon}{1 - \varepsilon} \quad (1)$$

where  $\varepsilon$  is the bed void fraction or effective porosity (dimensionless),  $\phi$  is the sphericity factor for the packing material (dimensionless), and  $d_p$  is the average particle diameter (m). The specific surface area of the channels,  $a_c$  (m<sup>2</sup>/m<sup>3</sup>) can be estimated by

$$a_c = \frac{n\pi d_c L}{AL} \quad (2)$$

where  $n$  is the number of channels (dimensionless),  $L$  is the bed height (m), and  $A$  is the cross-sectional area of the biofilter (m<sup>2</sup>).

### Estimation of Parameters

The specific surface area of the biofilter medium,  $a_0$  (m<sup>2</sup>/m<sup>3</sup>), can be estimated from the particle diameter,  $d_p$ , the void fraction, and the sphericity using the following equation:<sup>24</sup>

$$a_0 = \frac{6(1 - \varepsilon)}{\phi d_p} \quad (3)$$

Levenspiel<sup>25</sup> proposed an experimental method to estimate  $\phi$  using granulometry studies. The equation that relates  $\phi$  to  $d_p$  and the average wire sieve diameter,  $d_s$  (m), is

$$d_p \cong \phi d_s \quad (4)$$

where  $d_s$  is determined from the granulometry data using the following:<sup>25</sup>

$$d_s = \left[ \sum_i^m \frac{x_i}{d_i} \right]^{-1} \quad (5)$$

where  $d_i$  (m) is the average mesh size of the wire sieves where a mass fraction  $x_i$  (dimensionless) was caught.

The average particle diameter,  $d_p$ , can be estimated using pressure drop profiles and the quasi-empirical Ergun equation, which takes into account the dependence of viscous and kinetic energy losses on void fraction:<sup>26–28</sup>

$$\frac{\Delta P}{\rho} = \frac{150(1 - \varepsilon)^2 \mu U_0 L}{g_c \varepsilon^3 d_p^2 \rho} + \frac{1.75(1 - \varepsilon) U_0^2 L}{g_c \varepsilon^3 d_p} \quad (6)$$

where  $\Delta P$  is the pressure drop across the bed (cm of water [ $\text{H}_2\text{O}$ ]),  $g_c$  is the gravitational constant (1 kg m/sec<sup>2</sup> N),  $\mu$  is the air absolute viscosity ( $1.83 \times 10^{-5}$  kg/m sec),  $U_0$  is the superficial air velocity (m/sec), and  $\rho$  is the air density ( $0.927$  kg/m<sup>3</sup>). To obtain  $d_p$ , a pressure drop profile must be fit to eq 6 with the void fraction specified.

The void fraction,  $\varepsilon$ , in a porous media can be estimated using tracer studies with inert gases. The following equation can be used for analyzing the retention time distribution (RTD) curve for a step tracer input:<sup>29</sup>

$$t_r = \frac{\sum t_i C_{ii} \Delta t_i}{\sum C_{ii} \Delta t_i} \quad (7)$$

where  $t_r$  is the average gas retention time (sec);  $C_{ii}$  is the tracer concentration (mg/L) at a specified time  $i$ , and  $\Delta t_i$  is the difference between  $t_i$  and  $t_{i-1}$ . Considering the definition of retention time, the void fraction can be calculated using the average time calculated from eq 7 as follows:

$$\varepsilon = \frac{t_r Q}{AL} \quad (8)$$

where  $Q$  is the gas flow rate (L/min). This method has an advantage over the  $\text{H}_2\text{O}$  displacement technique in that it allows estimation of the void fraction without affecting the physical structure of the bed.

### Number of Particles and Channels

The number of channels in a packed bed,  $n$ , with particles whose form and arrangement are established by  $\varepsilon$ ,  $\phi$ , and  $d_s$  can be estimated by rearranging eqs 1, 2, 3 and 4 to yield

$$n = \frac{9(1 - \varepsilon)^2}{4 \varepsilon \phi^4} \left( \frac{d_T}{d_s} \right)^2 \quad (9)$$

where  $d_T$  is the biofilter diameter (m) considering that it is a cylinder. The number of particles ( $N$ ) in a bed can be estimated by dividing the volume of the solids by the average volume of a particle ( $V_p$ ):

$$N = \frac{AL(1 - \varepsilon)}{V_p} \quad (10)$$

where  $V_p$  is calculated using the equation for the volume of a sphere and eq 4. From this, the following equation is obtained to estimate the number of particles in a bed:

$$N = \frac{3(1 - \varepsilon)L}{2 \phi^3} \frac{d_T^2}{d_s^3} \quad (11)$$

### Linking Model Approaches

Internal changes in biofilter media physical structure that affect system performance occur over time. The proposed channel flow model can be used to estimate the changes in the number of particles, number of flow channels, average channel size, and specific surface area in a biofilter over time. The procedure is outlined in Table 1. Void fraction is determined both by tracer studies and by  $\text{H}_2\text{O}$  displacement only before biofilter operation to avoid saturating the bed while it is in operation.

## EXPERIMENTAL METHODS

### Experimental System

A system consisting of four identical bench-scale biofilter columns was used to treat  $\text{H}_2\text{S}$  in a moist air stream, as shown in Figure 1. Each of the columns (polyvinylchloride [PVC] columns, 0.101 m in diameter and 1.2 m in height) was filled to a height of 1 m with compost media. Each column had five gas and compost-sampling ports spaced 20 cm apart along the height of the media. The airflow rate was maintained at 10 L/min, which provided

**Table 1.** Relation among models for characterizing filter media.

Time	Step	Method	Parameter
Initial	1	Tracer studies (eqs 7, 8)	$\varepsilon$ , $t_r$
	2	Water displacement method	$\varepsilon$ (confirmed)
	3	Pressure drop studies with the Ergun equation (eq 6)	$d_p$
	4	Sieve tray analysis (eq 4)	$d_s$ , $\phi$
	5	Flow channel model (eqs 1, 3, 9, 11)	$d_c$ , $a_0$ , $n$ , $N$
Final	1	Tracer studies (eqs 7, 8)	$\varepsilon$ , $t_r$
	2	Pressure drop studies with the Ergun equation (eq 6)	$d_p$
	3	Sieve tray analysis (eq 4)	$d_s$ , $\phi$
	4	Flow channel model (eqs 1, 3, 9, 11)	$d_c$ , $a_0$ , $n$ , $N$

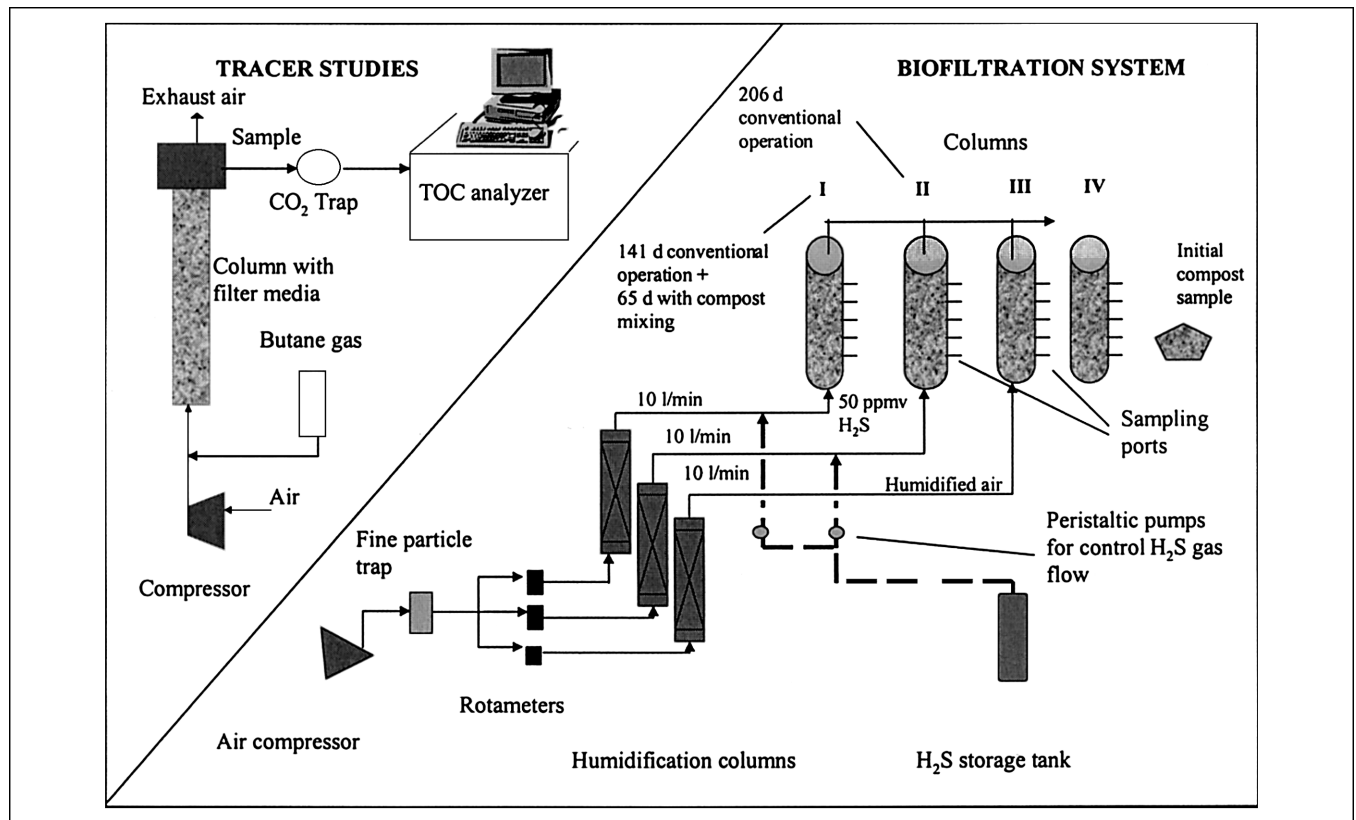


**Figure 1.** Experimental setup, tracer studies, and biofiltration system.

a superficial loading rate of  $74 \text{ m}^3/\text{m}^2/\text{day}$  with an empty bed residence time (EBRT) in each column of 50 sec. The air supply for the columns was controlled using a Cole Parmer mass flow controller and calibrated rotameters. The columns were operated in upflow mode. Compressed air (using a HAGEN-100 diaphragm compressor) was passed through three PVC humidification columns (0.15 m in diameter and 1.2 m in height) packed with 0.9 m of Rashig rings. The humidification columns provided close to 100% relative humidity.

A small controlled flow of  $\text{H}_2\text{S}$  from a gas cylinder was mixed with the main humidified airstream, which then was fed to the bottom of two of the columns (I and II), resulting in an  $\text{H}_2\text{S}$  concentration of 50 parts per million volume (ppmv) or  $4 \text{ g H}_2\text{S}/\text{m}^3/\text{hr}$ . A low loading of  $\text{H}_2\text{S}$  was chosen to avoid inhibition caused by sulfate ( $\text{SO}_4^{2-}$ ) accumulation. The third and fourth columns (III and IV) were used as controls. Only a humidified air stream was fed to column III. Neither  $\text{H}_2\text{O}$  nor gas was fed to column IV. The biofilter columns were located in a plastic enclosure on the roof of the Environmental Engineering Laboratory building at the barometric pressure of Mexico City (585 mm Hg) and at ambient temperature ( $20 \pm 5^\circ\text{C}$ ).

The biofilter media used was mature compost derived from food, leaf, and yard waste as well as horse manure. The compost was provided by the National University Compost Plant and was prepared in outdoor windrows.

The compost used for filling the biofilters was analyzed at the beginning of the experiment. Columns I, II, III, and IV were analyzed at the end of the experiment. Columns I and II were operated for 141 and 206 days, respectively, using conventional operating criteria. Media moisture content was controlled using  $\text{H}_2\text{O}$  addition at the top of the columns. Column I continued its operation for an additional 65 days (from day 142 until day 206), with media mixing every two days. Compost mixing was accomplished by removing the entire bed from the column, manually homogenizing the media, and then reincorporating it into the biofilter column. Less than 15 min was required for this operation. For the last 65 days of the experiment,  $\text{H}_2\text{O}$  was added to column I during the bed mixing procedure. The  $\text{H}_2\text{O}$  addition rate was based on a recommended  $\text{H}_2\text{O}$ -air ratio of between 1.5 and 3 mL  $\text{H}_2\text{O}$  per  $\text{m}^3$  of gas.<sup>30</sup> This resulted in a  $\text{H}_2\text{O}$  addition rate of 60 mL tap water every other day.

The  $\text{H}_2\text{S}$  concentration was measured in the inlet and along the length of the columns using electrochemical cells (SR11-U-100, BW Technologies). The cells were calibrated every 3 months using a known concentration (25 ppmv  $\text{H}_2\text{S}$ ) quality calibration/test gas (Lumidor calibration kit).  $\text{SO}_4^{2-}$  concentration, moisture content, and alkalinity were measured by removing small samples ( $\sim 1 \text{ g}$ ) of compost from each sample port. The  $\text{SO}_4^{2-}$  concentration in the filter media was measured by the

photometric method using Merck Spectroquant equipment (25 300 mg/L, 180 tests No. 114791). The moisture content of the compost was determined gravimetrically.<sup>31</sup> Alkalinity, sieve analysis, and pH of the biofilter media were measured using the method reported by Klute.<sup>32</sup> The sieve analysis was conducted using wet compost as obtained from the columns.

### Tracer Studies

Butane gas was used as tracer for determining the RTD curves because it has very low solubility (1.26 mM at 298 K)<sup>24</sup> and can be easily measured by the monitoring system. The tracer was injected into the columns using a pulse injection technique.<sup>29</sup> A continuous sample was collected, using a gas sampling pump, from the gas sampling ports of the biofilter to a carbon dioxide (CO<sub>2</sub>) detector (Beckman Industrial total organic carbon [TOC] analyzer, Model 915B). A CO<sub>2</sub> trap (potassium hydroxide [KOH], 1 M) in the tubing (located between the gas sampler and the TOC analyzer) was used to avoid interferences caused by CO<sub>2</sub> contained in the air. An automatic data recording system (Peaksimple II for SRI chromatographs) was connected to the TOC analyzer to reproduce the RTD curve on a screen and printer. Three tracer injections (1 mL each) per tracer study were performed, and an average RTD curve was determined. Mathematical analysis was performed using an Excel spreadsheet program to determine average gas retention time (eq 7). Each tracer study was carried out using an airflow rate of 10 L/min. To assure minimum interaction between the tracer input and compost, the compost was saturated with butane before each tracer study. This was carried out using a constant butane input into the inlet airstream until a constant butane concentration of 1.5 mg/L was reached in the biofilter outlet. This technique resulted in almost 100% recovery of the tracer when the RTD curves were analyzed. Saturation of the compost with butane also allowed

the calculation of a desorption curve. The butane loading was suddenly stopped, and the resulting desorption curve was used to calculate the quantity of butane sorbed to the compost. The difference between this value and the theoretical bed sorption capacity provided an additional estimate of the working void fraction in the bed.

### Pressure Drop

A profile of pressure drop versus gas flow rate for the biofilters was fit to the Ergun equation (eq 6) to determine the average particle diameter of the biofilter media as a function of height. The biofilters were subjected to airflows from 10 to 70 L/min in 10 L/min increments to obtain plots of pressure drop versus gas flow rate. An H<sub>2</sub>O differential manometer was used for pressure drop measurements. The effect of the fine screen and other equipment at the bottom of each column was corrected for by subtracting the pressure drop provided by those elements from each pressure drop measurement.

## RESULTS AND DISCUSSION

### H<sub>2</sub>S Removal and SO<sub>4</sub><sup>2-</sup> Control

H<sub>2</sub>S removal efficiency and compost media SO<sub>4</sub><sup>2-</sup> concentration for columns I and II are shown in Figure 2. Initial H<sub>2</sub>S removal efficiency approached 100% and decreased to ~90% over 206 days of operation. Column I had practically the same behavior as column II during the first 141 days. However, after compost mixing was initiated, the H<sub>2</sub>S removal efficiency was maintained at close to 100% in column I.

Media SO<sub>4</sub><sup>2-</sup> concentration stabilized at 10 and 21 mg SO<sub>4</sub><sup>2-</sup>-S/g dry compost for columns I and II, respectively. SO<sub>4</sub><sup>2-</sup> accumulation in the bed was caused by H<sub>2</sub>S oxidation to sulfuric acid (H<sub>2</sub>SO<sub>4</sub>). During the first 25 days of operation, the pH decreased from 7.5 to a stable value of 4.5 in both columns I and II. Degorce-Dumas et al.<sup>33</sup>

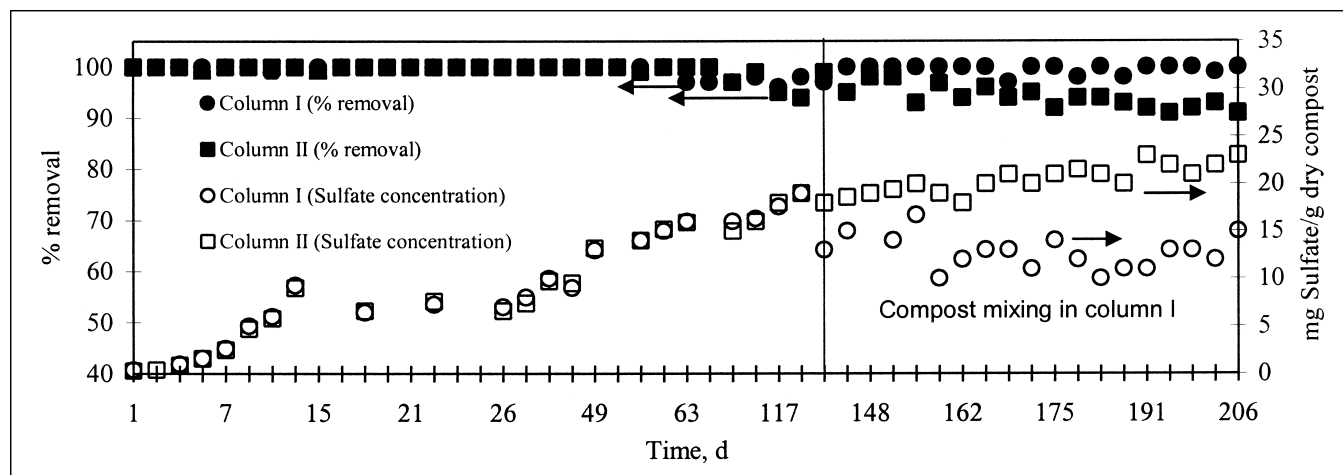


**Figure 2.** H<sub>2</sub>S removal efficiency and SO<sub>4</sub><sup>2-</sup> accumulation (mg SO<sub>4</sub><sup>2-</sup>-S/g dry compost) as a function of time with and without media mixing.

reported that this pH range is adequate for high H<sub>2</sub>S removal efficiencies. Similar observations were made by Wada et al.,<sup>34</sup> who reported H<sub>2</sub>S removal close to 100% using a peat biofilter at a controlled pH of 3.5.

SO<sub>4</sub><sup>2-</sup> accumulation could be an important factor in the decrease in H<sub>2</sub>S removal. Smet and Van Langenhove<sup>35</sup> noted that protons produced in a biofilter displaced nutrient cations (e.g., sodium [Na<sup>+</sup>], potassium [K<sup>+</sup>]) from the cation exchange sites on the compost material. The authors found that 95% of the SO<sub>4</sub><sup>2-</sup> was leached as the corresponding SO<sub>4</sub><sup>2-</sup> salts and not as H<sub>2</sub>SO<sub>4</sub>. As a result, essential nutrients were leached and the pH of the biofilter media remained low. As shown in Figure 2, the SO<sub>4</sub><sup>2-</sup> concentration in both biofilters was always lower than the inhibitory level of 25 mg SO<sub>4</sub><sup>2-</sup>-S/g dry compost reported by Yang and Allen.<sup>36</sup> Routine washing of the compost and compost mixing, in the case of column I, effectively mitigated SO<sub>4</sub><sup>2-</sup> accumulation.

Between days 74 and 102, operation was suspended because of a failure in the H<sub>2</sub>S flow control, and neither H<sub>2</sub>S nor H<sub>2</sub>O were supplied to the bed. Biofilter performance was practically unaltered even though the gas feed was stopped for 30 days. The biofilters recovered their normal H<sub>2</sub>S removal efficiency after 3 days, demonstrating the versatility of the biofilters under shutdown situations. This operational capacity of biofilters has also been reported by Zarook et al.<sup>10</sup>

### Changes in Physical Structure

The values determined for moisture content,  $d_p$ ,  $\epsilon$ ,  $\phi$ , and  $a_0$  for the initial compost sample as a function of biofilter height for all columns are shown in Table 2. The ratio between the values estimated by the flow channel model for the number of particles, number of channels, channel diameter, and specific surface area, and the initial compost characteristics for columns I, II, and III are shown in Figure 3.

**Table 2.** Experimental values for  $d_p$ ,  $\epsilon$ ,  $\phi$ ,  $a_0$ , and moisture content.

		Distance from Gas Inlet	$d_p$ (mm)	$\epsilon$	$\phi$	Compost Moisture (%)	$a_0^a$ (m <sup>2</sup> /m <sup>3</sup> )
Initial compost sample			1.9	0.4	0.81	65	2880
Column I	Conventional operation over 141 days	20	0.5	0.38	0.81	31	11,300
		40	0.7	0.37	0.80	35	8400
		60	1.2	0.34	0.81	40	5020
		80	1.4	0.49	0.82	51	3250
		100	1.9	0.44	0.81	71	2690
	Operation with compost mixing over 65 days	20	1.8	0.38	0.82	51	3070
		40	1.9	0.38	0.82	50	2910
		60	1.7	0.38	0.82	51	3250
		80	1.8	0.38	0.82	50	3070
		100	1.9	0.38	0.82	51	2910
Column II	Conventional operation over 206 days	20	0.5	0.39	0.81	30	11,150
		40	0.6	0.38	0.8	33	9680
		60	1.1	0.36	0.82	39	5190
		80	1.7	0.49	0.82	51	2670
		100	2.5	0.5	0.81	70	1820
Column III	Compost column with humidified air and water flow	20	0.5	0.39	0.82	31	10,880
		40	0.6	0.39	0.81	32	9290
		60	1.2	0.4	0.82	41	4460
		80	1.7	0.48	0.81	55	2790
		100	2.4	0.51	0.81	71	1860
Column IV	Compost column with no flow	20	2.1	0.39	0.81	51	2650
		40	2	0.4	0.82	52	2670
		60	2.1	0.39	0.82	51	2590
		80	1.9	0.38	0.82	50	2910
		100	1.9	0.38	0.82	50	2910

<sup>a</sup> $a_0$  was determined using eq 3.

**Particle Size.** Based on the average particle diameter (hereafter termed particle diameter) estimated by the pressure drop studies, there appeared to be an overall agglutination of particles in columns I, II, and III. Column I (under conventional operation) had an increase in particle diameter of ~73% (0.5–1.9 mm) over 141 days. The increase in particle diameter observed in column II (conventional operation) was close to 80% (0.5–2.5 mm) after 206 days. In both cases, a lack of media mixing resulted in a particle size distribution where the largest particles were located at the top of the column (gas outlet with H<sub>2</sub>O addition) and the smallest particles were at the bottom (gas inlet). The particle size distribution was closely associated with the moisture distribution. Dry compost with small particle sizes was located at the bottom of the columns and wet compost and large particle sizes were located at the top. The addition of H<sub>2</sub>O to the top of the column did not adequately control media moisture.

The constant distribution of particle size along the height of column I with media mixing is shown in Figure

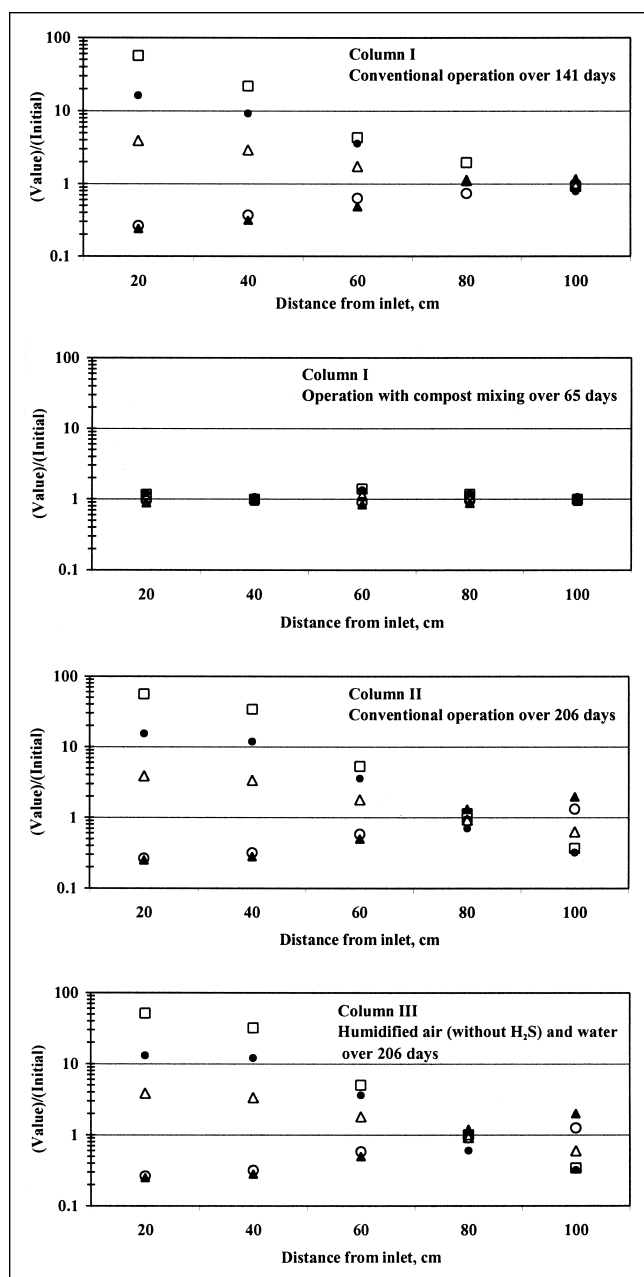


**Figure 3.** Ratio between the values estimated by the flow channel model for the number of particles,  $N$ ; number of channels,  $n$ ; channel diameter,  $d_c$ ; specific surface area,  $a_0$ ; particle diameter,  $d_p$ ; and the initial compost characteristics for columns I (both conventional and with media mixing), II, and III. Based on experimental  $d_p$ ,  $\epsilon$ , and  $\phi$  (see Table 2), it was calculated that  $N = 510,000$ ,  $n = 13,400$ ,  $d_c = 0.55$  mm, and  $a_0 = 2880$  m<sup>2</sup>/m<sup>3</sup> for the initial compost.

3. In this case, an average particle diameter of  $1.82 \pm 0.08$  mm was obtained, in contrast to the wide range obtained for conventional operation. Columns II (conventional operation) and III ( $H_2O$  + humidified air) had similar particle size, moisture, and void fraction distributions. This shows that biomass growth and elemental sulfur (S) accumulation did not influence the physical structure of compost as much as did airflow and humidification.

A small change was observed in particle diameter in the lower part (from 1.9 to 2.1 mm, 9.5%) for the biofilter column with no airflow (column IV) because of bed compaction by the bed weight itself. The difference between the initial and final column height was 6 cm. A similar amount of compaction was observed in columns II and III. Compaction in column I was completely avoided by media mixing.

**Sphericity.** The sphericity of the particles remained nearly constant ( $\sim 0.81 \pm 0.01$ ) throughout the experiment in all of the columns, as shown in Table 2. Neither particle agglutination nor particle disintegration changes the geometric form of the particles. This result is in agreement with Karamanev et al.,<sup>37</sup> who investigated the fractal structure of peat moss particles. They reported that a compost particle under magnification had a certain shape and when the magnification is increased, and one observes now a fragment of the first picture, the same shape can be observed, and so on. Because sphericity did not change significantly in compost, the granulometry test can be omitted from the procedure outlined in Table 1 after the initial characterization of the media.

**Void Fraction.** The initial void fraction of the compost was determined using both tracer studies and the water displacement method. The void fraction determined by the tracer study and water displacement method were 0.40 and 0.44 (9% difference), respectively, indicating that the void fraction estimated using tracer studies is the working void fraction rather than the entire void fraction available in the bed. The nonworking void fraction is the difference between the void fraction estimated by water displacement and tracer studies. The void fraction values reported in Table 2 were determined using tracer study measurements. The void fraction increased by 14 and 22% for columns I (conventional operation) and II, respectively. In column I with media mixing, the void fraction remained homogeneous at 0.38. The change in void fraction was closely related to changes in particle size, especially for the upper parts of the columns where  $H_2O$  was added.

**Pressure Drop.** A decrease in pressure drop was observed in column II (from 4.5 to 2.5 cm of  $H_2O$ ), probably because of the development of flow channels inside the filter media. Similarly, Allen and Phatak<sup>1</sup> and Allen and Yang<sup>6</sup> treating  $H_2S$  and methyl mercaptan emissions in compost biofilters, respectively, stated that the buildup in pressure drop may be suddenly released by channeling. Pressure drop distribution profiles showed a linear relationship of pressure drop with height in column I when compost mixing was carried out. For each 20 cm of column height,



an average pressure drop of  $0.89 \pm 0.16$  cm of H<sub>2</sub>O was measured.

**Number of Particles, Number of Flow Channels, and Specific Surface Area.** The initial compost sample and column IV (no airflow) had similar internal characteristics compared with the major changes observed in columns I and II, as shown in Figure 3. As discussed previously, under conventional operation, compost drying disintegrated the compost particles, producing a large number of particles and flow channels. The greatest difference was observed in the first section of column I (20 cm height, 0.101 m diameter). In this section, the number of particles was estimated at 29 million, with an average diameter of 0.5 mm. There were 218,000 flow channels with 0.13 mm diameter. The original compost had 510,000 particles with a diameter of 1.9 mm and 13,400 flow channels with 0.55-mm diameter. As expected, the specific surface area had a huge increase, from 2880 to 11,300 m<sup>2</sup>/m<sup>3</sup>. The moisture profile in column I indicates that it was operated under a drying process. Similar behavior can be observed (see Figure 3) for column II until the fourth section, which had 65 more days of conventional operation than column I. Even if the specific surface area was increased because of particle disintegration, the potential increase in H<sub>2</sub>S degradation was limited by a lack of moisture and microbial activity.

The fifth section of column II shows an inverse process may be occurring because of excess H<sub>2</sub>O addition. In this case, the particle diameter increased by 31% over the initial value. The number of particles and number of channels were 180,000 and 4300, respectively. In this case, the moisture content is higher than in the lower parts of the column; however, the specific surface area available for mass transfer decreased (1820 m<sup>2</sup>/m<sup>3</sup>). This specific surface area obtained by the flow channel model

agrees with the specific surface area estimated by Baltzis et al.<sup>38</sup> of 1900 m<sup>2</sup>/m<sup>3</sup> for a peat biofilter.

The effect of specific surface area reduction on biofilter removal capacity was quantified using the following first-order kinetic model based on convection-diffusion-reaction (CDR) phenomena presented by Ottengraf and Van den Oever:<sup>16</sup>

$$\frac{C_{ge}}{C_{go}} = \exp\left[-\frac{Da_0 LRT}{H_e U_0 \delta} \beta \operatorname{Tanh}(\beta)\right] \quad (12)$$

and

$$\beta = \sqrt{\frac{k\delta^2}{D}} \quad (13)$$

where  $C_{ge}$  is the effluent H<sub>2</sub>S concentration (mol/m<sup>3</sup>),  $C_{go}$  is the H<sub>2</sub>S concentration in the inlet gas stream (mol/m<sup>3</sup>),  $D$  is the diffusion coefficient in liquid phase (m<sup>2</sup>/sec),  $H_e$  is the Henry constant (m<sup>3</sup>/mol),  $T$  is the temperature (K),  $R$  is the ideal gases constant (Pa m<sup>3</sup>/mol/K),  $\delta$  is the biofilm thickness (m),  $k$  is the reaction rate constant (sec<sup>-1</sup>) and  $\beta$  is the Thiele number. This model was fit to the experimental data obtained from column I on day 206, when the column was working well under media mixing conditions, as shown in Figure 4. A biofilm thickness ( $\delta$ ) of 40 μm was assumed based on the range of 20–50 μm reported by Baltzis et al.<sup>38</sup> for a peat biofilter treating volatile organic compounds (VOCs). The H<sub>2</sub>S diffusivity in H<sub>2</sub>O is  $1.61 \times 10^{-9}$  m<sup>2</sup>/sec and the Henry constant is 880 m<sup>3</sup>/mol, both at a temperature of 20 °C.<sup>24</sup> The height of the bed was 1 m. The average specific surface area used was 3042 m<sup>2</sup>/m<sup>3</sup> based on the average of the five sections of the column. The reaction rate constant ( $k$ , sec<sup>-1</sup>) was calibrated based on the value, which minimized the

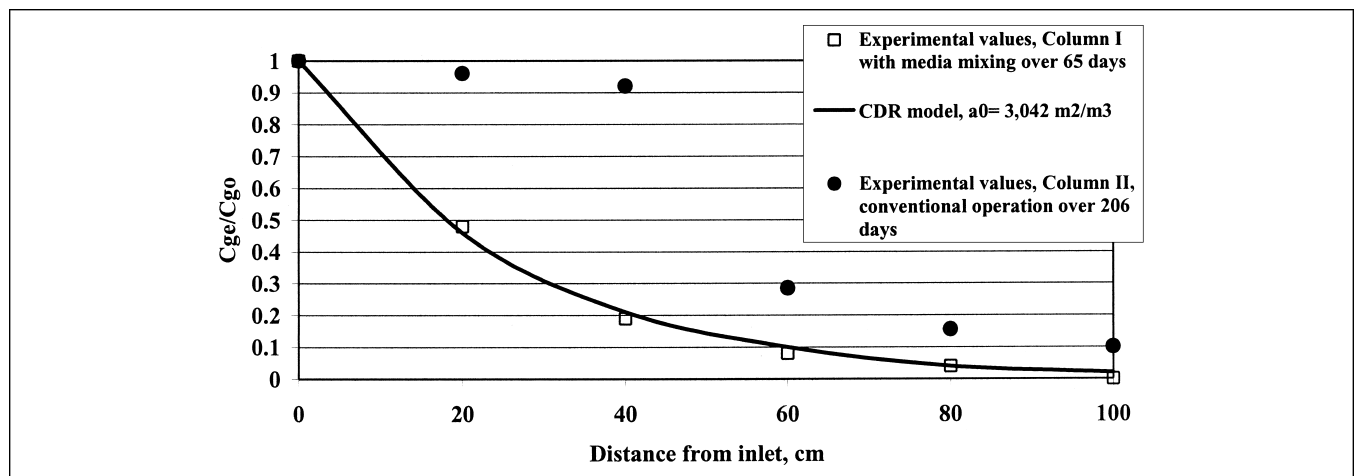


**Figure 4.** Experimental data from columns I and II on day 206 of operation as a function of biofilter height. Data from column I were fit to the C-D-R model.<sup>16</sup>  $C_{ge}$  = outlet H<sub>2</sub>S concentration;  $C_{go}$  = inlet H<sub>2</sub>S concentration.

residual sum of the squares of the error between the experimental and the model predicted concentrations. Under these conditions, a reaction rate constant of 0.26 sec<sup>-1</sup> was calibrated with a correlation coefficient of 0.998. With this calibration, eq 12 predicted a removal in each section of ~54%, which was in agreement with the experimental results obtained.

As shown in Figure 4, the H<sub>2</sub>S removal profile in column II was quite different from that in column I. Both media drying and changes in specific surface area can explain the changes in the removal profile. In the lower parts of the bed, the specific surface area increased; however, lack of moisture limited microbial activity, resulting in low H<sub>2</sub>S removal rates. In the upper parts of the bed, the moisture content was adequate for H<sub>2</sub>S degradation; however, channeling and the decrease in the specific surface area caused by particle agglutination limited removal. The presence of channels in the upper part of the column was observed visually. Deshusses and Cox<sup>39</sup> also observed channels in regions close to the walls of a column that were produced by airflow through a column media consisting of compost and wood scrap. In column I, H<sub>2</sub>S removal efficiency was maintained at close to 100% because compost mixing destroyed channels that were formed. The gas flowed through a wider conduit network with smaller diameter channels, which improved the interaction between the gas and the filter media, improving biofilter performance. This is in agreement with Schwarz et al.,<sup>40</sup> who found similar results applying a pore network model. The greatest removal efficiency (69%) was observed in the center of column II, at approximately the same loading rate as the first section of column I, which was in agreement with the theoretical result obtained by eq 12 (74%). This high removal efficiency can be explained by both the large specific surface area (5190 m<sup>2</sup>/m<sup>3</sup>) and the adequate moisture conditions (39%) in this section. This indicates that the best biofilter performance can be obtained in systems with high specific surface area and adequate moisture content.

**Gas Distribution.** The gas distribution in the biofilter media was quantified using tracer studies. The axial dispersion model response<sup>29</sup> for columns I, II, III, and IV and the initial sample are shown in Table 3. Figure 5 shows the RTD curves obtained for columns I and II at the end of the study. The RTD curves show plug flow behavior, which was analyzed using the following axial dispersion model:

$$\sigma_0^2 = 2\left(\frac{D_g}{U_0L}\right) - 2\left(\frac{D_g}{U_0L}\right)^2 (1 - e^{-[1/(D_g/U_0L)]}) \quad (14)$$

where  $D_g$  is the molecular diffusivity in the gas phase (m<sup>2</sup>/sec), and  $\sigma\theta^2$  is the normalized variance (dimensionless).

**Table 3.** Axial dispersion number model response.

Column	Description	Axial Dispersion Number, $D_g/U_0L \cdot 10^{-3}$ (dimensionless)
Sample	Initial compost	10.7
I	End of conventional operation	8.5
I	End of study, with media mixing	10.8
II	End of study, conventional operation	8.4
III	With humidified air and water flow	8.4
IV	Neither water or air-H <sub>2</sub> S	10.7

Eq 7 was used to calculate the average retention time,  $t_r$ , and the following expression was used for the variance:<sup>29</sup>

$$\sigma^2 = \frac{\sum t_i^2 C_{ti} \Delta t_i}{\sum C_{ti} \Delta t_i} - t_r^2 \quad (15)$$

The normalized variance ( $\sigma\theta^2$ ) was calculated by dividing the variance (eq 15) by the square of the average time,  $t_r$  ( $\sigma\theta^2 = \sigma^2/t_r^2$ ).<sup>29</sup>

The term  $D_g/U_0L$  in eq 14 is called the axial dispersion number and is the inverse of the Peclet number. It can be used to access the dispersion intensity within the system. A widely accepted value for the axial dispersion number to define plug-flow or well-mixed behavior is not available in the literature. However, complete mixing can be expected as the axial dispersion number increases.<sup>29</sup>

In columns I, II, and III (see Table 3), a decrease in the axial dispersion number was observed at the end of conventional operation, which implies reduced gas mixing. This can be explained by channeling and consequent dead zone formation. The term dead zone accounts for the portion of the medium where the fluid is stagnant. The average residence time for columns I and II were 19.1 and 17.6 sec, respectively, indicating a dead zone in column II of ~8%.

Gas channel formation is influenced by gas flow rate, moisture content, and type of biofilter media used. Pressure drop, as well as gas distribution and media moisture, can be controlled when media mixing is used. As shown in Table 3, when media mixing was performed in biofilter I, gas distribution remained constant, avoiding channel formation. The axial dispersion number at the end of the operations in biofilter I remained constant and close to the initial value.

Information about gas interaction inside the media was also provided by the butane desorption curves. At the end of each tracer study, the butane dosage was suddenly interrupted. The butane concentration at the column outlet decreased slowly because absorbed butane was desorbing. The sorbed quantity of butane was calculated

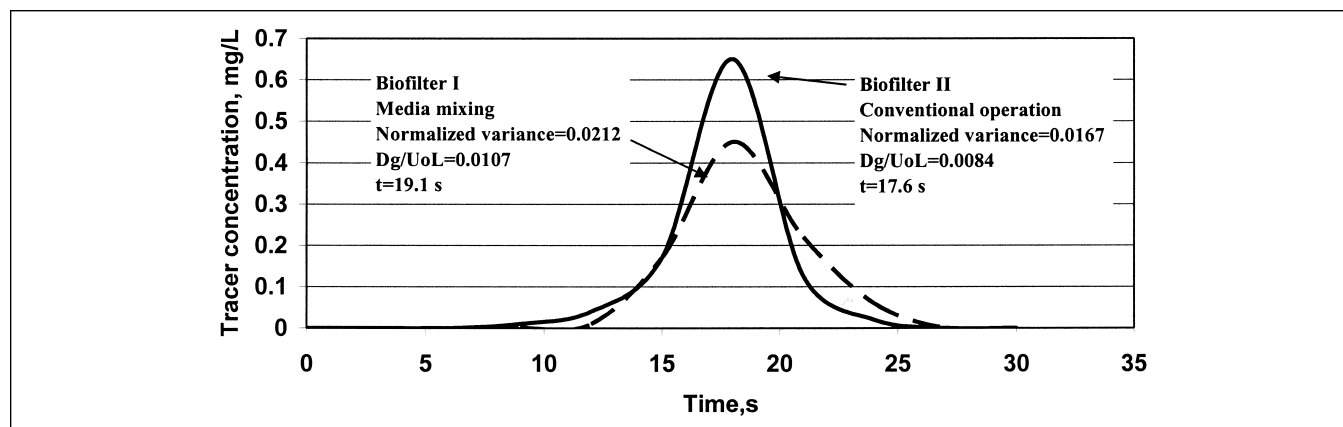


**Figure 5.** RTD curves obtained for biofilter II at the end of conventional operation and for biofilter I at the end of the compost mixing phase.

by integration of the area under each curve and multiplying by the gas flow used (10 L/min). Taking into account the solubility of butane in H<sub>2</sub>O (1.26 mM), the bulk density of compost (0.59 kg/L), and the moisture content (50%), the quantity of butane that could be sorbed in the 8.01 L of compost was estimated at 172 mg. The mass of butane sorbed was 151 and 171 mg for conventional operation and compost mixing, respectively. This shows that there is a dead zone of ~12% in column II that was not in contact with the tracer. This value is similar to the dead zone found using tracer studies, which was 8%. The desorption curve also showed the importance that media mixing has on gas distribution in the medium.

## CONCLUSIONS

An analysis technique was proposed to estimate the changes in physical structure that a biofilter medium, such as compost, undergoes as a function of time in a biofiltration system. This experimental technique applied information from tracer studies, granulometry, and pressure drop analysis to a model that estimates number of channels, average channel diameter, number of particles, and specific surface area. The H<sub>2</sub>S initial removal efficiency for a conventionally operated biofilter decreased from 100 to 90% over 206 days of operation. Column II had practically the same behavior as column I over the first 141 days; however, when compost mixing was carried out, the H<sub>2</sub>S removal efficiency was maintained at near 100%. Variations in moisture content and specific surface area can explain experimental results that show this decrease in H<sub>2</sub>S removal as a function of time.

The internal changes that occurred in the biofilters over time are closely related to moisture conditions inside the biofilter. The conventionally operated biofilters had significant internal changes, especially in the lower part of each biofilter, because of the compost drying. Compost drying resulted in a large number of disintegrated compost particles and flow channels. The greatest

difference was observed in the first section of each biofilter, where the gas inlet was located. To avoid flow channel formation, as well as to achieve constant media moisture, particle size and gas distribution, void fraction, and general homogeneity, it is recommended that media mixing be carried out with controlled H<sub>2</sub>O addition. Routine washing of the compost and compost mixing effectively mitigated SO<sub>4</sub><sup>2-</sup> accumulation and kept the compost at an adequate moisture content of ~50%.

## ACKNOWLEDGMENTS

The authors acknowledge financial support from the Mexican National Council for Science and Technology (CONACyT, Proy. 27776-B). Morgan-Sagastume was supported by a fellowship from the American Chemical Society, Academia Mexicana de Ciencias, Fundación México-Estados Unidos para la Ciencia, for a summer stay at the University of Massachusetts, Amherst, MA.

## REFERENCES

- Allen, E.R.; Phatak, S. Control of Organosulfur Compound Emissions Using Biofiltration. Methyl Mercaptan. In *Proceedings of the 86th Annual Conference & Exhibition of A&WMA, Denver, CO, June 1993*; A&WMA: Pittsburgh, PA, 1993.
- Alonso, C.; Suidan, M.T.; Sorial, G.A.; Smith, F.L.; Biswas, P.; Smith, P.J.; Brenner, R.C. Gas Treatment in Trickle-Bed Biofilters: Biomass, How Much Is Enough?; *Biotechnol. Bioeng.* **1997**, *54*, 583-594.
- Acuña, M.E.; Pérez, F.; Auria, R.; Revah, S. Microbiological and Kinetic Aspects of a Biofilter for the Removal of Toluene from Waste Gases; *Biotechnol. Bioeng.* **1999**, *63*, 175-184.
- Chitwood, D.E.; Devinsky, J.S.; Meiburg, E. Heterogeneous Flow through Biofilter Media. In *Proceedings of the 93rd Annual Conference & Exhibition of A&WMA, Salt Lake City, UT, June 2000*; A&WMA: Pittsburgh, PA, 2000.
- Lacey, J.A.; Brady, D.L.; Apel, W.A. Comparison of NO<sub>x</sub> Removal Efficiencies in Compost Based Biofilters Using Four Different Compost Sources. In *Proceedings of the 94th Annual Conference & Exhibition of A&WMA, Orlando, FL, June 2001*; A&WMA: Pittsburgh, PA, 2001.
- Allen, E.R.; Yang, Y. Biofiltration Control of Hydrogen Sulfide Emissions. In *Proceedings of the 84th Annual Conference & Exhibition of A&WMA, Vancouver, British Columbia, Canada, June 1991*; A&WMA: Pittsburgh, PA, 1991.
- Chung, Y.C.; Chihpin, H.; Ching-Ping, T. Microbial Oxidation of Hydrogen Sulphide with Biofilter; *J. Environ. Sci. Health* **1996**, *6*, 1263-1278.
- Sabo, F.; Motz, U.; Fisher, K. Development and Testing of High Efficiency Biofilters. In *Proceedings of the 86th Annual Conference & Exhibition of A&WMA, Denver, CO, June 1993*; A&WMA: Pittsburgh, PA, 1993.

9. Van Lith, C.; Leson, G.; Michelsen, R. Evaluating Design Options for Biofilters; *J. Air & Waste Manage. Assoc.* **1997**, *47*, 37-48.
10. Zarook, S.M.; Shaikh, A.A.; Ansar, Z. Development, Experimental Validation and Dynamic Analysis of a General Transient Biofilter Model; *Chem. Eng. Sci.* **1997**, *52*, 759-773.
11. Wubker, S.M.; Laurenzis, A.; Werner, U.; Friedrich, C. Controlled Biomass Formation and Kinetics of Toluene Degradation in a Bioscrubber and in a Reactor with Periodically Moved Trickle-Bed; *Biotechnol. Bioeng.* **1997**, *55*, 686-692.
12. Auria, R.; Frere, G.; Morales, M.; Acuña, M.E.; Revah, S. Influence of Mixing and Water Addition on the Removal Rate of Toluene Vapors in a Biofilter; *Biotechnol. Bioeng.* **2000**, *68*, 448-455.
13. Morgan-Sagastume, F.; Sleep, B.E.; Allen, D.G. Effects of Biomass Growth on Gas Pressure Drop in Biofilters; *J. Environ. Eng.* **2001**, *127*, 388-396.
14. Bohn, H. Consider Biofiltration for Decontaminating Gases; *Chem. Eng. Prog.* **1992**, *April*, 34-40.
15. Higuchi, T.; Okazawa, S.; Kinoshita, H.; Sakamoto, T. A New Design for Biological Treatment of Gaseous Pollutants: Biofiltration of Hydrogen Sulfide Using Parallel-Moving Biosheet. In *Proceedings of the 94th Annual Conference & Exhibition of A&WMA, Orlando, FL, June 2001*; A&WMA: Pittsburgh, PA, 2001.
16. Ottengraf, S.P.P.; Van den Oever, A.H.C. Kinetics of Organic Compound Removal from Waste Gases with a Biological Filter; *Biotechnol. Bioeng.* **1983**, *25*, 3089-3102.
17. Kirchner, K.; Hauk, G.; Rehm, H.J. Exhaust Gas Purification Using Immobilized Monocultures (Biocatalysts); *Appl. Microbiol. Biotechnol.* **1987**, *26*, 579-587.
18. Abumaizar, R.J.; Smith, E.H.; Kocher, W. Analytical Model of Dual Media Biofilter for Removal of Organic Air Pollutants; *J. Environ. Eng.* **1997**, *123*, 606-614.
19. Zarook, S.; Baltzis, B.C.; Oh, Y.S.; Bartha, R. Biofiltration of Methanol Vapor; *Biotechnol. Bioeng.* **1993**, *41*, 512-524.
20. Shareefdeen, Z.; Baltzis, B.S. In *Advances in Bioprocesses Engineering*; Galindo, E., Ramirez, T., Eds.; Kluwer Acad. Press: Dordrecht, The Netherlands, 1994; pp 397-404.
21. Deshusses, M.A.; Hamer, G.; Dunn, I.J. Behavior of Biofilters for Waste Air Biotreatment. 1. Dynamic Model Development; *Environ. Sci. Technol.* **1995**, *29*, 1048-1058.
22. Dullien, F.A.L. *Porous Media: Fluid Transport and Pore Structure*; Academic: San Diego, CA, 1992.
23. McCabe, W.L.; Smith, J.C.; Harriott, P. *Unit Operations of Chemical Engineering*; McGraw Hill International Edition: New York, NY, 1993.
24. Perry, R.H.; Green, D. *Perry's Chemical Engineers Handbook*; McGraw-Hill International: New York, NY, 1988.
25. Levenspiel, O. *Engineering Flow and Heat Exchange*; Plenum Press: New York, 1998.
26. Ergun, S. Fluid Flow through Packed Columns; *Chem. Eng. Prog.* **1952**, *48*, 89-94.
27. Gostomski, P.A.; Liaw, L.P. Air Permeability of Biofilter Media. In *Proceedings of the 94th Annual Conference & Exhibition of A&WMA, Orlando, FL, June 2001*; A&WMA: Pittsburgh, PA, 2001.
28. Madamba, P.S.; Driscoll, R.H.; Buckle, K.A. Bulk Density, Porosity and Resistance to Airflow of Garlic Slices; *Drying Technol.* **1994**, *12*, 937-954.
29. Levenspiel, O. *Chemical Reaction Engineering*; John Wiley: New York, 1972; pp 253-325.
30. Leson, G.; Winer, A.W. Biofiltration: An Innovative Air Pollution Control Technology for VOC Emissions; *J. Air & Waste Manage. Assoc.* **1991**, *41*, 1045-1054.
31. Parent, L.E.; Caron, J. In *Soil Sampling and Methods of Analysis*; Carter M., Ed.; Canadian Society of Soil Science; Lewis Publishers: Manitoba, Canada, 1993; pp 441-458.
32. Klute, A. *Methods for Soil Analysis*; American Society of Agronomy, Soil Science Society of America: Madison, WI, 1986; p 12-2.6.5.
33. Degorce-Dumas, J.R.; Kowal, S. Le Cloirec, P. Microbial Oxidation of Hydrogen Sulphide in a Biofilter; *Can. J. Microbiol.* **1997**, *43*, 264-271.
34. Wada, A.; Shoda, M.; Kubota, H.; Kobayashi, T.; Katayama-Fujimura, Y.; Kuraishi, H. Characteristics of H<sub>2</sub>S Oxidizing Bacteria Inhibiting a Peat Biofilter; *J. Ferment. Technol.* **1986**, *64*, 161-167.
35. Smet, E.; Van Langenhove, H. Abatement of Volatile Organic Sulfur Compounds in Odorous Emissions from the Bio-industry; *Biodegradation* **1998**, *9*, 273-284.
36. Yang, Y.; Allen, E.R. Biofiltration Control of Hydrogen Sulfide I. Design and Operational Parameters; *J. Air & Waste Manage. Assoc.* **1994**, *44*, 863-868.
37. Karamanev, D.G.; Bélanger, M.C.; Chavarie, C.; Chaouki, J.; Mayer, R. Hydrodynamic Characteristics of a Trickling Bed of Peat Moss Used for Biofiltration of Wastewater; *Can. J. Chem. Eng.* **1994**, *72*, 411-416.
38. Baltzis, B.C.; Wojdyla, S.M.; Zarook, S.M. Modeling Biofiltration of VOC Mixtures under Steady-State Conditions; *J. Environ. Eng.* **1997**, *123*, 599-605.
39. Deshusses, M.A.; Cox, H.H.J. The Use of CAT Scanning to Characterize Bioreactors for Waste Air Treatment. In *Proceedings of the 91st Annual Conference & Exhibition of A&WMA, San Diego, CA, June 1998*; A&WMA: Pittsburgh, PA, 1998.
40. Schwarz, B.C.E.; Nukunya, T.; Devinny, J.S.; Tsotsis, T.T. A Pore Network Model of Biofilter Clogging. In *Proceedings of the USC-TRG Conference on Biofiltration*, Los Angeles, CA, October 10-20, 2000; pp 167-174.

#### About the Authors

Juan M. Morgan-Sagastume is a Ph.D. student and research assistant, and Adalberto Noyola is a researcher and subdirector of the Institute of Engineering at National Autonomous University in Mexico City, Mexico. Sergio Revah is a head researcher in the Processes and Hydraulics Department at Metropolitan Autonomous University in Iztapalapa, Mexico. Sarina J. Ergas is an associate professor in the Department of Civil and Environmental Engineering at the University of Massachusetts in Amherst, MA. Address correspondence to: Juan M. Morgan-Sagastume National Autonomous University, Apdo. Postal 70-472, Coyoacán, 04510, Mexico City, Mexico; fax: (5255) 5616-27-98; e-mail: jmms@pumas.iingen.unam.mx.